Narrow-leafed lupin (Lupinus angustifolius L.): Characterization of emulsification and fibre properties

Arzami, Anis

2022-09-29

Arzami , A , Morais de Carvalho , D , Vilaplana , F , Stoddard , F & Mikkonen , K S 2022 , ' Narrow-leafed lupin (Lupinus angustifolius L.): Characterization of emulsification and fibre properties ' , Future Foods , vol. 6 , 100192 . https://doi.org/10.1016/j.fufo.2022.100192

http://hdl.handle.net/10138/349577
https://doi.org/10.1016/j.fufo.2022.100192

Future Foods 6 (2022) 100192

Contents lists available at ScienceDirect

Future Foods

journal homepage: www.elsevier.com/locate/fufo

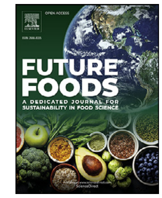

Narrow-leafed lupin (*Lupinus angustifolius* L.): Characterization of emulsification and fibre properties

Anis N. Arzami[a,*], Danila Morais de Carvalho[a], Francisco Vilaplana[b,c], Frederick L. Stoddard[d,e], Kirsi S. Mikkonen[a,e]

[a] *Department of Food and Nutrition, PO Box 66, 00014, University of Helsinki, Finland*
[b] *Division of Glycoscience, Department of Chemistry, KTH Royal Institute of Technology, AlbaNova University Centre, 106 91 Stockholm, Sweden*
[c] *Wallenberg Wood Science Centre, KTH Royal Institute of Technology, 100 44 Stockholm, Sweden*
[d] *Department of Agricultural Sciences and Viikki Plant Science Centre, PO Box 27, 00014, University of Helsinki, Finland*
[e] *Helsinki Institute of Sustainability Science (HELSUS), PO Box 65, 00014, University of Helsinki, Finland*

A R T I C L E I N F O

Keywords:
Lupin
Fibre structure
Physicochemical properties
Suspension
Emulsion

A B S T R A C T

Lupin is among the most promising plant-based food protein sources due to its high protein and fibre content. The fibre fraction, especially from seed coats, is often seen as low in value (discarded as waste or as animal feed) and greater knowledge on its composition and structure are crucial to increase its usefulness. However, only one model of lupin fibre structure exists in the literature. Our sample of Finnish-grown narrow-leafed lupin seed consisted of fibre (43.3%), protein (31.3%), fat (8.1%) and starch (0.2%). According to the sugar analysis, rhamnogalacturonan-I, with branches of arabinan and galactan, constituted the main pectin population in the fibre fraction. A revised model of the overall fibre structure is proposed. At concentrations of 0.75% and 1.0%, both unrefined and defatted flour of whole lupin seeds produced stable suspensions and oil-in-water emulsions, demonstrating their application as potential emulsifiers. This study presents the knowledge and opportunity to support sustainability through the utilization of whole lupin seed for future industrial applications.

1. Introduction

The agricultural lupins (*Lupinus albus* L., *L. angustifolius* L. and *L. luteus* L.) are important potential sources of protein for food and feed uses (Lucas et al., 2015). They are adapted to cool-temperate agriculture and, as legumes, are capable of biological nitrogen fixation in symbiosis with appropriate bacteria in the Rhizobiaceae, so they can be grown with minimal use of fertilizer nitrogen. Their grain protein content is high (global averages of 38%, 34% and 42% of seed dry matter, respectively; Feedipedia, 2022) and the biological value of white lupin protein, for example, is 91% of that of egg albumin protein (Egaña et al., 1992). Nevertheless, the value of plant protein is seldom enough in itself to make a legume crop profitable, especially if the grain is used for feed purposes, and other sources of value need to be developed (De Visser et al., 2014). The lupins are challenging in this respect, because they store germination energy in thickened cell walls (22–24% of seed dry matter) (Feedipedia, 2022) rather than as oil (5–10% of seed dry matter) or starch (<1% of seed dry matter). The composition of this cell-wall fraction is not well characterized so its potential uses are not well developed. The functional properties of the protein and fibre (e.g., solubility, foaming, emulsification and gelation) provide an important path for increasing the economic value of lupin seeds.

Lupin proteins have been isolated by many procedures (Lqari et al., 2002; Sironi et al., 2005; Jayasena et al., 2011; Süssmann et al., 2013; Berghout et al., 2014) and their physico-chemical properties (Pollard et al., 2002; Raymundo et al., 2002; Berghout et al., 2015a; Lo et al., 2021) and bioavailability (Mariotti et al., 2007; Porres et al., 2007; Lammi et al., 2016) have been investigated. In comparison, the fibre fractions have been less studied, with most focus being on the seed-coat fraction rather than the cotyledon fraction (Miao et al., 2001; Turnbull et al., 2005; Zhong et al., 2018; Zhong et al., 2019). In the dehulling process, up to 31% of the dry matter of the whole seed is lost in the seed coats and adhering parts of the cotyledons, and most goes to either waste or animal feed (Sipsas, 2008; Zhong et al., 2018) with only limited uses in food (e.g., high fibre bakery products and meat products)

Abbreviations: FFS, Full-fat lupin flour suspension; DFS, Defatted lupin flour suspension; FFE, Full-fat lupin flour emulsion; DFE, Defatted lupin flour emulsion; UT, Ultra-Turrax (high-speed homogenizer); MF, Microfluidizer (high-pressure homogenizer); d_{32}, Surface mean diameter; d_{43}, Volume mean diameter; TSI, Turbiscan stability index; SD, Standard deviation; HG, Homogalacturonan; RG, Rhamnogalacturonan; XG, Xylogalacturonan; ISM, Industrial-scale microfluidizer.

* Corresponding author.
E-mail address: anis.arzami@helsinki.fi (A.N. Arzami).

https://doi.org/10.1016/j.fufo.2022.100192
Received 7 March 2022; Received in revised form 7 September 2022; Accepted 21 September 2022

(Tucek, 2006; LupinFoods, 2022). In order to minimize these losses, it is desirable to utilize the whole lupin seed.

The main components in the cell walls of the lupin seeds are described as beta-galactans, which therefore constitute the main potential dietary fibre (Buckeridge et al., 2000). The existing model shows the structure of the beta-galactan, together with arabinans, to be neutral branches from a rhamnogalacturonan backbone. The main galactan is β-(1→4) linked and a secondary form is β-(1→3), (1→6) linked, while α-(1→5) arabinan is also present. The model was developed using data from hydrolysis of the cell wall fraction by endogenous enzymes in germinating seeds of narrow-leafed lupin (*L. angustifolius*) (Buckeridge et al., 2000). Use of more modern techniques would provide greater detail on this structure that could indicate ways of making different and profitable uses of the fibre fraction.

For these reasons, we set out to investigate the chemical composition of lupin fibre fraction and to elucidate its structure. Furthermore, we characterized the solubility, water-holding capacity, viscosity, physical stability and microstructure of flour milled from the whole lupin seed (full-fat and defatted). The results provided indications of potential new high value uses of the lupin crop.

2. Materials and methods

2.1. Materials

Untreated, fully ripe and dry seeds of narrow-leafed lupin were purchased from Koivunalhon Luomutila, Tarvasjoki, Finland. The Dietary Fibre Kit, Total Starch Assay Kit, high purity MES monohydrate [2-(N-morpholino)ethanesulfonic acid] buffer salt (B-MES 250) and Celite were obtained from Megazyme, Ireland. Isopropanol (99.5%) and heptane were supplied by Fisher Scientific, UK. Ethanol (99.5%) was supplied by Altia Oyj, Finland. Rapeseed oil was purchased from a local supermarket. All chemicals and reagents used in this work were of analytical grade.

2.2. Preparation of flours

Lupin seeds were milled with a ZM-200 ultra-centrifugal mill (Retsch, Germany, sieve pore size 0.5 mm) into full-fat fine flour. The mill speed was set at 8000 rpm and the batch size was 200 g. The particle size (d_{32}) of the full-fat flour was 56.1 ± 2.2 μm. Half of the full-fat flour was used to prepare defatted flour (d_{32} = 43.5 ± 1.1 μm) as described below. Both full-fat and defatted flours were stored at 4 °C until use.

2.3. Chemical and structural characterization

2.3.1. Fat content determination and preparation of defatted lupin flour

Full-fat flour was subjected to organic extraction for the determination of the fat content and for preparing defatted flour. Samples of 5 g of full-fat lupin flour was weighed into cellulose extraction thimbles and placed in a Soxtec apparatus (Soxtec Avanti 2050). About 80 mL of the solvent mixture (heptane:isopropanol, 3:2 (v/v)) was placed in a pre-weighed metallic cup holder, heated to its boiling point and continuously recirculated for the remaining extraction time. The following parameters were used: temperature 170 °C, boiling time 45 min, rising time 30 min, recovery time 10 min, and warm-up time 1 min. The defatted flour was collected and dried in a fume hood for subsequent chemical characterization and emulsion preparation. The fat content was determined gravimetrically after solvent evaporation. Six replicates were prepared.

2.3.2. Dietary fibre determination

Defatted lupin flour was subjected to sequential enzymatic hydrolyses for the determination of dietary fibre and preparation of lupin fibre for analysis using the Megazyme Total Dietary Fibre (TDF) kit following the manufacturer's instructions. The only modification was that a filter bag with porosity of 50 μm was used instead of a crucible covered with Celite for filtering the sample after enzymatic hydrolyses, to facilitate sample recovery and avoid Celite contamination of the fibre used for monosaccharide, protein and ash analyses. The dietary fibre determination was performed in duplicate using a blank for correcting any contribution from reagents to the dietary fibre result using standard Megazyme TDF procedures.

2.3.3. Protein determination

Protein content of full-fat and defatted flour samples was calculated from the nitrogen moiety determined in duplicate according to the Dumas combustion method on a Leco 828 CN analyzer (Leco Inc., St Joseph, MI, USA). The nitrogen moiety in the fibre fraction (used for the correction of the value of the dietary fibre content) was determined by the Kjeldahl method (using a 2300 Kjeltec Analyzer unit - Ordior) after acid mineralization. The standard factor of 6.25 was used for converting the nitrogen content into protein content.

2.3.4. Ash content determination

Ash content was determined in duplicate samples by ashing a 1-g sample at 525 °C in a muffle furnace for 6 h. For the correction of the dietary fibre, the ash was mineralized by adding 2 mL of concentrated nitric acid and drying it in a sand bath at 60 °C, ashing again and weighing the residue.

2.3.5. Monosaccharide composition

The monosaccharide composition of the fibre fraction was assessed by gas chromatography (GC) after acid methanolysis according to Sundberg et al. (1996). A local calibration curve was prepared using standard monosaccharides. Analysis was performed in triplicate.

2.3.6. Starch content determination

The starch content of the full-fat flour and fibre fraction were determined on duplicate samples with the Megazyme Total Starch Assay kit according to the manufacturer's instructions.

2.3.7. Moisture content determination

One-gram samples of full-fat flour, defatted flour and fibre fraction were weighed and dried overnight at 105 °C in a drying oven (Termaks TS 8000, Termaks AS, Norway). The samples were re-weighed and the moisture content was used to correct flour composition to a dry-matter basis.

2.3.8. Glycosidic linkage analysis

The glycosidic linkage pattern in lupin fibre was assessed using gas chromatography coupled with mass spectrometry (GC-MS) after derivatization and hydrolysis of the polysaccharides into permethylated alditol acetates (PMAAs). The preparation of the PMAAs involves swelling of the lupin fibre in dimethyl sulfoxide with SO_2 and diethylamine, methylation in alkali conditions with methyl iodide, hydrolysis, reduction and acetylation (Albersheim et al., 1967; Ciucanu et al., 1984). PMAAs were separated and analyzed according to Morais de Carvalho et al. (2017). The glycosidic linkage analysis was performed in triplicate.

2.3.9. Fourier transform infrared (FTIR) spectroscopy

FTIR spectra from full-fat flour, defatted flour and fibre fraction were recorded at room temperature using a Perkin-Elmer FTIR spectrometer equipped with a universal attenuated total reflection (ATR) sampling accessory according to the following parameters: 4000–600 cm^{-1} wavelength; 16 scans; 4 cm^{-1} resolution; at intervals of 1 cm^{-1}. Baseline correction and normalization (at 1600 cm^{-1}) were applied as post-treatment to the spectra. Only one spectrum was collected for each sample.

2.3.10. Nuclear magnetic resonance (NMR) spectroscopy

About 30–40 mg of fibre was suspended in 700 μL deuterated water (D_2O) overnight under agitation (room temperature). The proton NMR analysis was carried out using a Bruker Advance 850 Hz III high-definition spectrometer equipped with a cryoprobe (Bruker Corp., MA) according to the following parameters: Bruker pulse program zgpr (with pre-saturation to remove the water signal from spectra), size of FID of 32768, total of 2 dummy scans and 32 scans. Existing databases were used in the assignments for proton resonances (Rosenbohm et al., 2003; Winning et al., 2007; Morais de Carvalho et al., 2017).

2.4. Preparation of aqueous suspensions and emulsions of flour

Full-fat (FFS) and defatted flour (DFS; both at 0.25%, 0.5%, 0.75% and 1%, w/v concentrations) suspensions were prepared by wetting the samples with ethanol and addition of hot milliQ-water (80 °C). Suspensions were vigorously mixed and heated at 80 °C for 2 h. A subset of these heat-treated suspensions was homogenized at 22 000 rpm for 2 min in an Ultra-Turrax T25 (UT; Ika-Werke, Staufen, Germany). A subset of these homogenized suspensions was further treated with a microfluidizer 110Y (Microfluidics, Westwood, MA, USA; high-pressure homogenization, MF, 4 passes, 800 bar) at room temperature to produce a fine solution. All suspension samples were adjusted to pH 7 using a few drops of 1 M NaOH. Full-fat flour emulsion (FFE) and defatted flour emulsion (DFE) were prepared by mixing the unhomogenized suspensions (pH 7) with rapeseed oil (5%, w/v) before homogenization by UT and MF as described above.

2.5. Water solubility and water-holding capacity

Water solubility and water-holding capacity of lupin flours with different processing treatments (non-heated, heat-treated, and heat-treated with homogenization) were determined based on the method from Zhong et al. (2019). Briefly, FFS and DFS (1%, w/v) were wetted with ethanol and magnetically stirred with water (50 mL) for 2 h. In the case of heat-treated samples, hot water was added and the samples were heated at 80 °C for 2 h with continuous stirring. Some of the heat-treated samples were further homogenized with UT (22 000 rpm, 2 min) only or a combination of UT and MF. After treatment, each sample was transferred into a tube and centrifuged (Hermle Z323 centrifuge, Hermle Labortechnik GmbH, Wehingen, Germany) at 3000 × g, 25 °C for 20 min. The supernatant was discarded and the tube containing the precipitate was inverted and left to drain for 15 min. The fresh weight of the precipitate was determined and water-holding capacity was expressed as the water retained by precipitate divided by the weight of dry starting material (g water/g flour). The precipitate was dried at 100 °C for 24 h, weighed and the percentage of solubility was calculated by dividing the loss of sample weight by the weight of the dry starting material. Triplicates were performed for each sample.

2.6. Particle size measurement

The droplet size distribution, surface mean diameter (d_{32}) and volume mean diameter (d_{43}) of the particles in suspension and oil droplets in emulsion were determined using a Mastersizer 3000 static light scattering apparatus mounted with a Hydro EV dispersion accessory (Malvern Instruments Ltd, Malvern, UK) controlled using the Mastersizer v.3.62 (Malvern Instruments Ltd.) application software. Each sample was gently shaken a few times before the analysis. The refractive index of rapeseed oil and the dispersion medium were set at 1.47 and 1.33, respectively. Every measurement was performed in triplicate.

2.7. ζ-potential measurement

The ζ-potential of suspension (FFS and DFS) and emulsion (FFE and DFE) samples after treatments were determined using an electrophoretic light scattering instrument (Zetasizer Nano ZS series, Malvern Instruments Ltd). Before measurement, all samples were diluted to 0.001% particle/ droplet concentration using Milli-Q water to avoid multiple scattering effects. The diluted sample was then added into the folded capillary cell (DTS1070 cell, Malvern Instruments Ltd.), which had two electrodes. The cell was inserted into the instrument, then equilibrated at 25 °C for 120 s. Three measurements were obtained from the instrument and ζ-Potential was calculated based on the Smoluchowski model on the acquired electrophoretic data using Dispersion Technology Software v. 5.10 (Malvern Instruments). Every measurement was performed in triplicate.

2.8. Viscosity measurement

The viscosity of suspension (FFS and DFS) and emulsion (FFE and DFE) samples after treatment was determined using a rheometer (Haake Rheostress 600, Thermo Electron GmbH, Germany) with a cone and plate geometry (35 mm diameter, 2° cone angle). The measurement was done using a stepwise rotation program with a shear rate ranging from 1 s^{-1} to 100 s^{-1} and 100 s^{-1} to 1 s^{-1} at 20 °C. The viscosity values of the samples at the shear rate of 10 s^{-1} were compared. Every measurement was performed in triplicate.

2.9. Physical stability

About 20 mL of each of the suspension (FFS and DFS) and emulsion (FFE and DFE) samples was poured into a transparent glass vial and kept at room temperature undisturbed. The physical stability of the samples was measured by Turbiscan Lab Expert analyzer (Formulaction, Toulouse, France). The vials were vertically scanned from the bottom to the top by a near-infrared light (λ = 880 nm) source during the measurement. The intensity of transmitted (at 180°) and backscattered light (at 45°) were measured simultaneously by the detectors. The Turbiscan stability index (TSI) was calculated using the Turbiscan software (v. 1.2) based on the changes in backscattering values during storage over the sample height. An increase of TSI over time indicates a decrease of sample stability. Photographs of the samples were taken every day up to one week of storage at room temperature.

2.10. Microstructure of suspension and emulsion

A light microscope (AxioVision, Carl Zeiss, Microimaging GmbH, Jena, Germany) connected with an AxioCam MRm digital camera (Carl Zeiss) was used to observe the microstructure of the flour suspension (FFS and DFS) and emulsion (FFE and DFE) samples. A drop of the prepared sample was placed in the middle of a microscope slide, covered with a cover slip and observed at 40 × magnification. Images were acquired using AxioVision v.4.7.1.0 (Carl Zeiss) application software.

2.11. Statistical analysis

All experiments were repeated at least twice and expressed as the mean ± standard deviation (SD), unless otherwise specified. The measurements were performed on duplicate samples. All statistical analyses and the significant differences ($p < 0.05$) were evaluated via SSPS 13.0 software using one-way ANOVA and Tukey's test.

3. Results and discussion

3.1. Chemical composition of lupin seeds and structural model of their fibre

The proximal composition of the narrow-leafed lupin seeds (Fig. 1A) was similar to that previously obtained in Finland (Lizarazo et al., 2015), where the protein content was 33%, fibre content 43%, lipid content 7%, ash content 4% and starch content 0.7%. These nutritional attributes

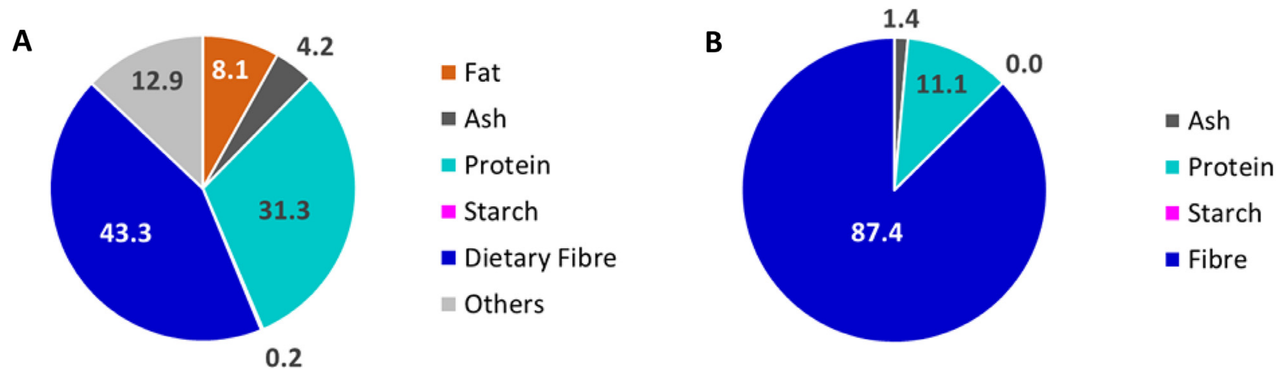

Fig. 1. Chemical composition of full fat flour of narrow-leafed lupin (A) and dietary fibre from the defatted flour (B).

Table 1
Monosaccharide composition and glycosidic linkage analysis of dietary fibre from defatted flour of narrow-leafed lupin. Gray rows indicate structural units found mainly in pectin.

Linkage	Structural units deduced	Average, % mol (SD)
t-Ara*f*	Ara*f*-(1 →	4.6 (2.4)
t-Ara*p*	Ara*p*-(1 →	0.5 (0.2)
2-Ara*f*	→ 2) Ara*f*-(1 →	0.2 (0.0)
3-Ara*f*	→ 3) Ara*f*-(1 →	0.0 (0.0)
5-Ara*f*	→ 5) Ara*f*-(1 →	8.2 (0.5)
3,5-Ara*f*	→ 3,5) Ara*f*-(1 →	0.1 (0.0)
2,5-Ara*f*	→ 2,5) Ara*f*-(1 →	7.2 (0.3)
2,3,5-Ara*f*	→ 2,3,5) Ara*f*-(1 →	0.5 (0.1)
Total Ara		**21.4 (3.6)**
t-Rha*p*	Rha*p*-(1 →	0.4 (0.3)
2,4-Rha*p*	→ 2,4) Rha*p*-(1 →	1.4 (0.1)
Total Rha		**1.8 (0.4)**
t-Gal*p*	Gal*p*-(1 →	3.1 (0.9)
3-Gal*p*	→ 3) Gal*p*-(1 →	0.5 (0.2)
2-Gal*p*	→ 2) Gal*p*-(1 →	0.1 (0.1)
4-Gal*p*/4-Gal*p*A[a]	→ 4) Gal*p*-(1 → or → 4) Gal*p*A-(1 →	48.5 (4.0)
6-Gal*p*	→ 6) Gal*p*-(1 →	0.2 (0.1)
3,4-Gal*p*	→ 3,4) Gal*p*-(1 →	0.1 (0.1)
2,4-Gal*p*	→ 2,4) Gal*p*-(1 →	0.6 (0.2)
4,6-Gal*p*	→ 4,6) Gal*p*-(1 →	1.5 (0.3)
Total Gal/GalA		**54.5 (5.7)**
t-Xyl*p*	Xyl*p*-(1 →	1.2 (0.6)
4-Xyl*p*	→ 4) Xyl*p*-(1 →	9.5 (0.3)
2,4-Xyl*p*	→ 2,4) Xyl*p*-(1 →	0.3 (0.1)
Total Xyl		**10.9 (1.0)**
t-Man*p*	Man*p*-(1 →	0.5 (0.1)
4-Man*p*	→ 4) Man*p*-(1 →	1.0 (0.6)
3,4-Man*p*	→ 3,4) Man*p*-(1 →	0.3 (0.1)
4,6-Man*p*	→ 4,6) Man*p*-(1 →	0.6 (0.3)
Total Man		**2.4 (1.0)**
t-Glc*p*	Glc*p*-(1 →	0.2 (0.1)
4-Glc*p*	→ 4) Glc*p*-(1 →	7.4 (0.3)
4,6-Glc*p*	→ 4,6) Glc*p*-(1 →	1.4 (0.1)
Total Glc		**9.0 (0.5)**

[a] Galactose and galacturonic acid contents of 43.4% and 11.1%, respectively. Values estimated according to the ratio of 4.38 for Gal/GalA obtained by monosaccharide analysis (Supporting Information, Table S1). Figures in brackets show standard deviation.

make lupin seeds an attractive candidate in the formulation of plant-based protein-rich food, particularly dietetic foods with a high dietary fibre content (Sujak et al., 2006). Earlier studies have shown that the high ash content of lupin includes nutritionally valuable amounts of calcium, magnesium, manganese, iron, zinc, and copper (Lizarazo et al., 2016; Mohammed et al., 2017).

The dietary fibre fraction was about one-ninth protein (Fig. 1B). The main polysaccharide was identified as a pectin containing both homogalacturonan (HG) (linear and unbranched region) and rhamnogalacturonan (RG) I (branched region) domains (Table 1 and Fig. 2).

The identification of pectin structure was supported by the identification of the glycosidic linkage. Both the GalA content from monosaccharide analysis and the results from linkage analysis (4-GalA) confirmed the presence of a large fraction of unsubstituted galacturonic acid (11.1%) attributed to the HG domain. Similarly, the RG I domain was consistent with the substitution pattern observed in rhamnosyl units (2,4-Rha*p*), in which linkages at positions 1 and 2 are associated to the typical formation of RG I backbone and those at position 4 corroborated with the side chain substitutions (Harholt et al., 2010). Moreover, the presence of β-(1,4)-galactan and α-(1,5)-arabinan substitutions at position 4 of rhamnosyl units was confirmed by the relative abundance of the corresponding glycosidic linkages. The β-(1,4)-galactan was identified as the main side chain in RG I domain due to the abundance of galactose identified by chemical analysis (43.4%).

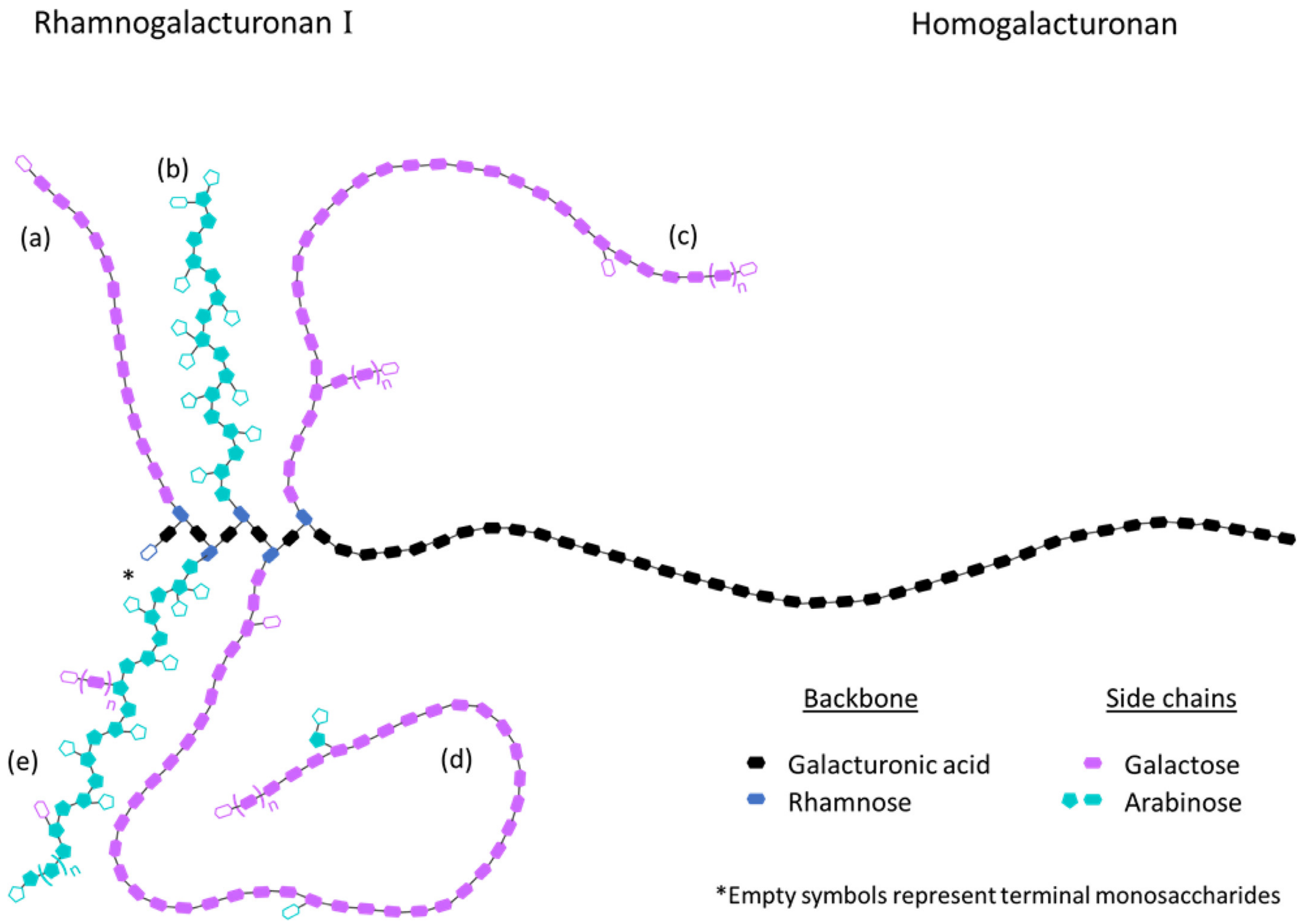

Fig. 2. Empirical structures of pectin domains identified in fibre of narrow-leafed lupin, based on 50 monosaccharide units in the backbone. Structural possibilities for side chains include linear galactan (a), branched arabinan substituted only by terminal arabinosyl units (b), branched galactan substituted only by terminal galactosyl units and/or galactan (c), branched arabinan substituted also by terminal galactosyl units and/or short-length galactan (d), and branched galactan substituted also by terminal arabinosyl unit and/or short-length arabinan (e). Note that n in galactan substitutions represents the number of galactosyl units, which can be either few or many.

Other minor polysaccharide populations from xylan, mannan, and cellulose groups were also identified in the fibre fraction. Although the substitution of galacturonic acid in pectin backbone by terminal xylosyl units (t-Xyl) has been reported to be responsible for forming a xylogalacturonan (XG) region in some species (Harholt et al., 2010; Byg et al., 2012), these were not found in the present study. The substantial amount of xylosyl moiety (10.9%) in the sample and, especially, the identification of 1→4 xylosyl (4-Xyl) (9.5%) units, typical for xylan backbone, supported the occurrence of long and low-substituted xylan chains in the composition of the lupin fibre.

Galactomannan in seeds performs a storage function and especially in the Fabaceae is important for its role in controlling water and imbibition in the early stages of germination (Buckeridge et al., 2000). Glycosidic linkage analysis revealed the presence of a population of galacto(gluco)mannan with low abundance (1–2%), supported by the presence of unsubstituted 4-Man*p* units and substituted Man*p* units at the 3- (3,4-Man*p*) and 6- positions (4,6-Man*p*), putatively with terminal galactosyl (t-Gal) substitutions (Table 1). Therefore, it is expected that 0.6% of t-Gal identified in the sample are involved in galactomannan substitutions (Table 1).

A certain amount of unsubstituted glucosyl units (4-Glc*p*) probably arising from cellulose (7.6%) was also identified (Table 1), in which the strong hydrolysis enabled the disruption of cellulose crystallinity and its complete assessment. When only mild hydrolysis was performed for monosaccharide assessment through methanolysis, cellulose crystallinity was preserved, so glucose content was likely underestimated then (Table S1, Supporting Information).

Certain features of the structure of the pectin were estimated by the combination of the results of monosaccharide analysis and glycosidic linkage analysis (Table 2) and this structural information was integrated to propose an empirical model for the pectin structure in narrow-leafed lupin seed (Fig. 2). Therefore, monosaccharide moieties from xylan, mannans, and cellulose populations were not considered in such calculations. The high ratio of galactose to galacturonic acid (Gal/GalA: 4.38), together the linkage pattern of galactosyl units and ratio of unsubstituted galactosyl units versus branching points (Table 2) suggested the existence of a long β-(1,4)-galactan side chain in the RG I domain. These findings were also supported by the high value obtained for the length of the side chain (36.0) in the RG I domain, in which the α-(1,5)-arabinan side chain was also accounted. Although pectin in lupin seed contains long side chains, such branches were observed restricted to the RG I domain (0.16 mole ratio). In the RG I domain, the Rha/GalA ratio was 1:1, while the remaining GalA moieties were involved in the formation of the HG domain (Fig. 2).The linkage analysis revealed moderate branching of the galactan side chains, with approximately 19 unsubstituted 4-Gal*p* units for every branching point. Results from linkage

Table 2
Structural features of the pectin population obtained from the combination of results from monosaccharide analysis (GC) and glycosidic linkage analysis (GC-MS) of dietary fibre isolated from narrow-leafed lupin.

Parameters	Mole ratio
Gal/GalA[a]	4.38
Rha/GalA[b]	0.16
(Gal + Ara)/Rha[c]	36.0
GalA/(Ara + Rha + Gal)[d]	0.17
4-Gal/(3,4-Gal+2,4-Gal+4,6-Gal)[e]	18.8
5-Ara/(3,5-Ara+2,5-Ara+2,3,5-Ara)[f]	1.0

[a] Ratio between galactose and galacturonic acid obtained from monosaccharide analysis used to differentiate the 4-Gal*p*/4-Gal*p*A (Table 1) into galactose and galacturonic acid moieties. Results from monosaccharides analysis are presented in Table S1 (Supporting Information).
[b] Portion of the pectin that corresponds to the RG I domain (Zhi et al., 2017).
[c] Length of the side chain linked to the RG I domain (Zhi et al., 2017).
[d] Pectin linearity (Zhi et al., 2017).
[e] Ratio of unsubstituted Gal units versus branching points.
[f] Ratio of unsubstituted Ara units versus branching points.

analysis supported the possibility of the occurrence of terminal galactosyl and arabinosyl moieties, short- and long-length galactan, and short-length arabinan substitutions in galactan side chains. These patterns of substitutions are in accordance with previous studies on pectin structure from different plant sources (Buckeridge et al., 2000; Øbro et al., 2004; Harholt et al., 2010; Byg et al., 2012). Conversely, the arabinan side chains were heavily substituted with one unsubstituted arabinosyl unit (5-Ara) per branching point. In the arabinan side chain, substitutions due to terminal arabinosyl and galactosyl moieties and short-length galactan were also consistent with previous results for various plant sources (Øbro et al., 2004; Harholt et al., 2010; Byg et al., 2012). The variation in certain chemical and structural parameters of pectin from different sources, such as branch patterns (number and size) and degree of substitution (acetylation and methylation) directly impacts on the technological properties of pectin, for example its gelling ability (Thakur et al., 1997; Øbro et al., 2004; Harholt et al., 2010; Byg et al., 2012). Furthermore, the extraction process may also cause some modification of pectin structure. Therefore, to assess the suitability of the pectin prepared here and characterized for the preparation of stable suspension and emulsion, specific experiments were conducted and the discussion is presented below (Section 3.2).

FTIR analysis of the full fat flour, defatted flour, and dietary fibre (Fig. 3) showed a broad band at 3282 cm^{-1}, due to hydroxyl stretching vibration in polysaccharides (Sun et al., 2004; Thambiraj et al., 2018) in all samples, but in a lower intensity in the defatted flour. The band at 2925 cm^{-1} indicated the C–H stretching vibration in polysaccharides (Sun et al., 2004; Thambiraj et al., 2018). The band due to the presence of acetyl groups in the full-fat sample, observed at 1743 cm^{-1} (Bian et al., 2010), was reduced following the sample processing and only a small shoulder was observed in the dietary fibre sample, indicating that deacetylation occurred.

Even after protease digestion, some residual protein remained in the fibre (Fig. 1B) and it was probably bound to polysaccharides. In support of this hypothesis, a set of bands was used for the identification of protein bonded to polysaccharides, at 1641 cm^{-1} (due to amide I), 1540 cm^{-1} (due to amide II) and 1399 cm^{-1} (due to amide III) (Thambiraj et al., 2018) (Fig. 3). The intensity of these bands decreased from the full fat sample to the dietary fibre, indicating protein removal from the sample. The band at 1245 cm^{-1}, due to the C–O stretching and the sharp band at 1055 cm^{-1}, due to C–O, C–C stretching or C–OH bending in monosaccharide units was also identified (Chaikumpollert et al., 2004; Xu et al., 2010), confirming the structure of the polysaccharide. The band at 896 cm^{-1} is attributed to β-glycosidic linkages between the various monosaccharides identified in the pectin structure

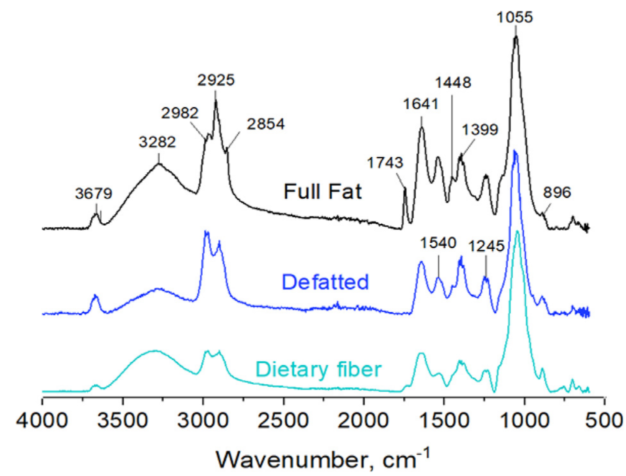

Fig. 3. FTIR spectra of full fat flour, defatted flour and dietary fibre isolated from narrow-leafed lupin. The following structures were identified: hydroxyl (3282 cm^{-1}); C-H (2925 cm^{-1}); acetyl groups (1743 cm^{-1}); protein bonded to polysaccharides due to amide I (1641 cm^{-1}), amide II (1540 cm^{-1}), and amide III (1399 cm^{-1}); C–O (1245 cm^{-1}); C–O, C–C or C–OH (1055 cm^{-1}); and β-glycosidic linkages (896 cm^{-1}).

and other polysaccharide moieties such as xylan, mannan, and cellulose (Gupta et al., 1987; Yang & Zhang, 2009).

The solubilization of lupin fibre in D_2O for ^{1}H NMR analysis was only partial and since preliminary tests using temperature during the solubilization (80 °C) showed no improvement in the solubility of the sample, the solubilization step was performed at room temperature. The signal at δ_H 5.12 (Fig. 4) was indicative of an anomeric proton (H-1). The region at δ_H 5.20–5.00 is also indicative of the presence of methylation at H-1, in which highest degree of methylation leads to a shifting of the signal downfield (Rosenbohm et al., 2003). According to the signal obtained for lupin fibre, if pectin is methylated, the degree of substitution is likely low. Small signals observed at δ_H 5.11-5.00 also suggested the presence of traces of carboxylic acid (–COOH; δ_H 5.11) and methyl acetate (–COOCH$_3$; δ_H 5.06) (Winning et al., 2007). Other attributes of the pectin structure regarding to anomeric proton at H-5, H-4, H-3, and H-2 were identified at δ_H 4.80-4.60, δ_H 4.44-4-36 (slight shoulder), δ_H 3.98, and δ_H 3.70-3.68 (sharp signals), respectively (Rosenbohm et al., 2003; Winning et al., 2007). The small signals at δ_H 2.00-2.25 were indicative of the presence of residual acetyl groups (CH$_3$–CO–) bonded to polysaccharides (Morais de Carvalho et al., 2017), supporting the FTIR results that indicated a small band in the spectrum of dietary fibre (Fig. 3) resulting from the deacetylation that occurred during the fibre isolation procedure.

3.2. Physical characterization of lupin flours

Water solubility values of FFS and DFS were ~40% and ~35%, respectively, when both suspensions were stirred at room temperature (2 h) or heat-treated at 80 °C for 2 h (Fig. 5A). The water-holding capacity of DFS was slightly higher (~6 g_{H2O}/g_{flour}) than FFS (~5 g_{H2O}/g_{flour}) when both samples were heated (80 °C) for 2 h (Fig. 5B).

The water solubility of FFS and DFS samples was not affected by heat treatment and was marginally higher after high-speed homogenization (UT) treatment, but was greatly increased by microfluidization, particularly in the case of the DFS (Fig. 5A). The water-holding capacity of DFS increased slightly with homogenization (UT; ~6.5 g_{H2O}/g_{flour}), but that of FFS decreased slightly (UT; ~4.9 g_{H2O}/g_{flour}). The combination of UT and MF treatments greatly increased the water-holding capacity of both heat-treated FFS and DFS. These results relate to the potential cooking quality of the lupins.

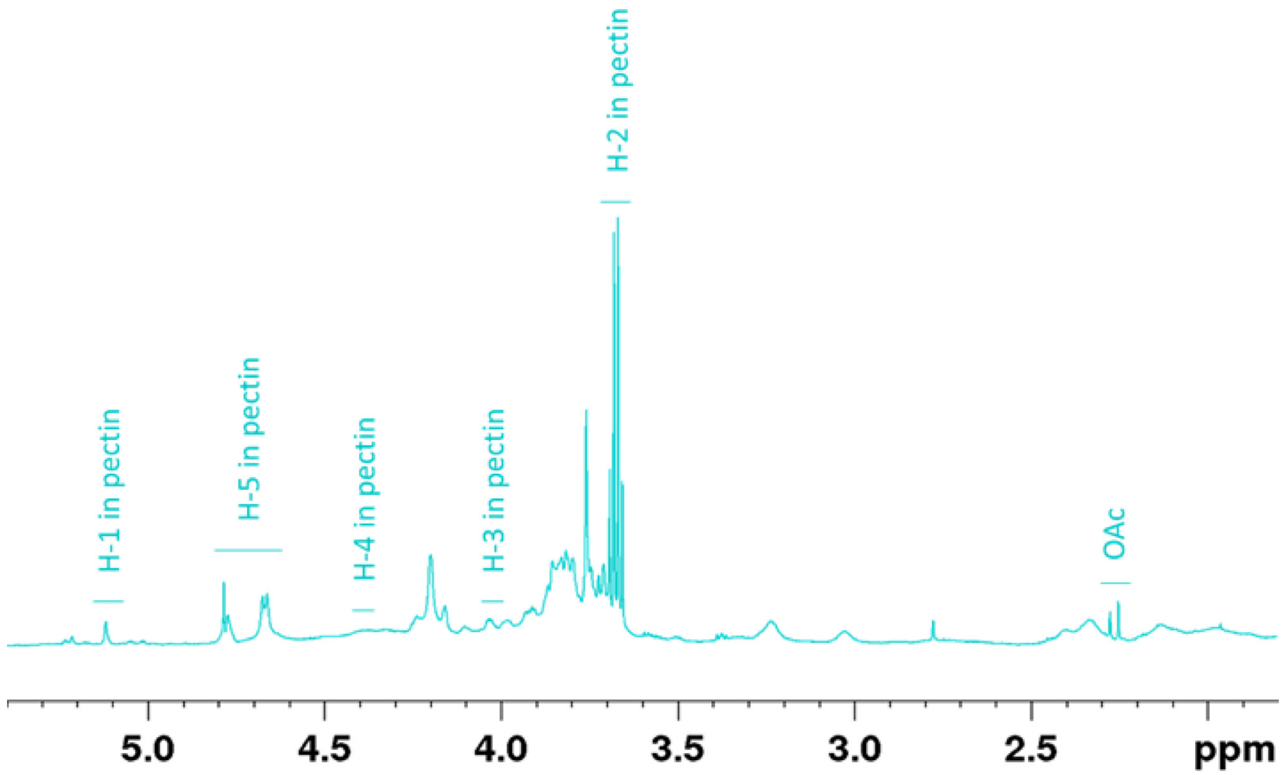

Fig. 4. [1]H NMR spectrum of dietary fibre isolated from narrow-leafed lupin. The presence of anomeric proton at the position 1 (H-1), 2 (H-2), 3 (H-3), 4 (H-4), and 5 (H-5) was confirmed. Small signals due to the presence of residual acetyl groups (OAc) were also identified.

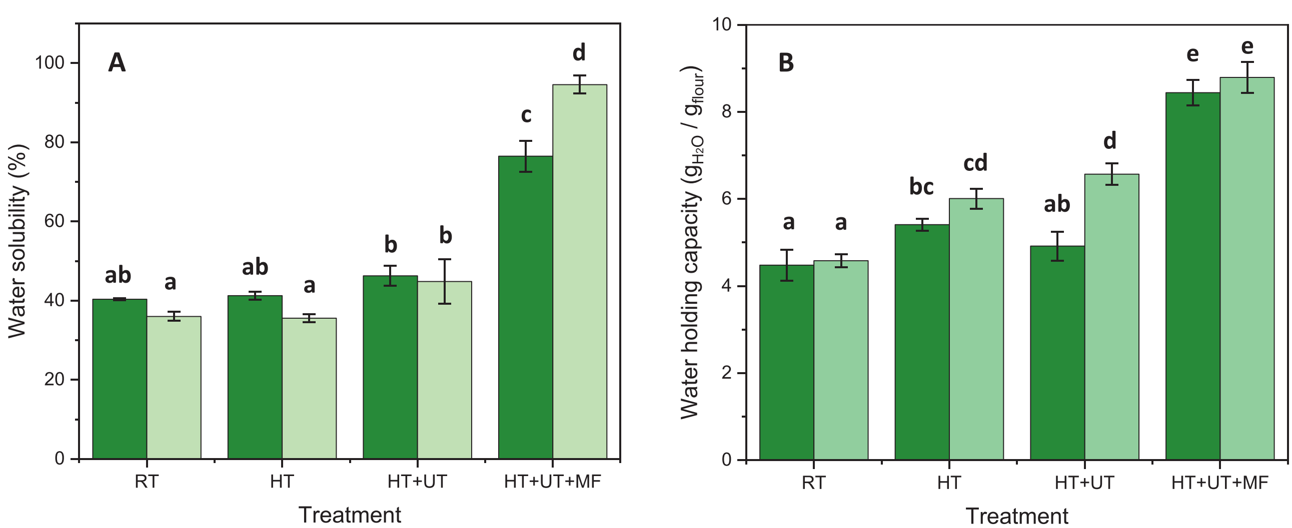

Fig. 5. (A) Water solubility of full-fat flour suspension (FFS, dark green) and defatted flour suspension (DFS, light green) of narrow-leafed lupin. (B) Water holding capacity of full-fat flour suspension (FFS, dark green) and defatted flour suspension (DFS, light green). RT = room temperature; HT = heat treatment at 80 °C for 2 h; UT = Ultra-Turrax (high-speed homogenization); and MF = microfluidization (high-pressure homogenization). Vertical error bars represent the standard deviation of the means (*n = 3*). Different lowercase letters in the figures indicate significant differences ($p < 0.05$) according to Tukey's HSD.

The results showed that both water solubility and water-holding capacity of the insoluble part of lupin fibre can be enhanced by using mechanical treatments such as high-speed and high-pressure homogenization. These treatments disrupt the cell wall structures, fragment the particles and unwrap them, increasing the surface activity of the flour, so more water interface can be stabilized (Joseph et al., 2020). Extrusion cooking can also be used to increase the solubility of the insoluble lupin fibre (Zhong et al., 2019; Naumann et al., 2021). In the present study, DFS had a higher capability to absorb water than FFS. Similarly, defatted lupin flours showed greater water (18%) and oil (103%) absorption than full-fat flours (Sathe et al., 1982), due to the increased availability of water-binding sites that were previously blocked by the lipophilic environment.

For the preparation of oil-in-water emulsions of FFS and DFS, the flour concentrations (0.25%, 0.5%, 0.75% and 1.0%) were chosen based on the suggestion by Peng et al. (2016) and Sridharan et al. (2020) that protein molecules in concentrations between 0.2% and 0.3% are sufficient to cover the water or emulsion interface. Higher protein concentration is not preferred as it thickens the suspension and emulsion systems (Sridharan et al., 2020), and since the samples contained the seed coats,

Table 3
Composition of emulsions made with different concentrations of flour from narrow-leafed lupin.

Lupin flour (%)	Lupin flour (g)	Water (g)	Oil (g)	Oil (%)	Sample to oil ratio (SOR)	Estimated protein concentration (%)*	
						Full fat (FFE)	Defatted (DFE)
0.25	0.38	142.13	7.5	5	0.05	0.078	0.082
0.50	0.75	141.75	7.5	5	0.10	0.156	0.164
0.75	1.13	141.38	7.5	5	0.15	0.234	0.245
1.00	1.50	141.00	7.5	5	0.20	0.313	0.327

*Estimated protein concentration (%) was calculated from the protein content of full-fat and defatted lupin flour samples.

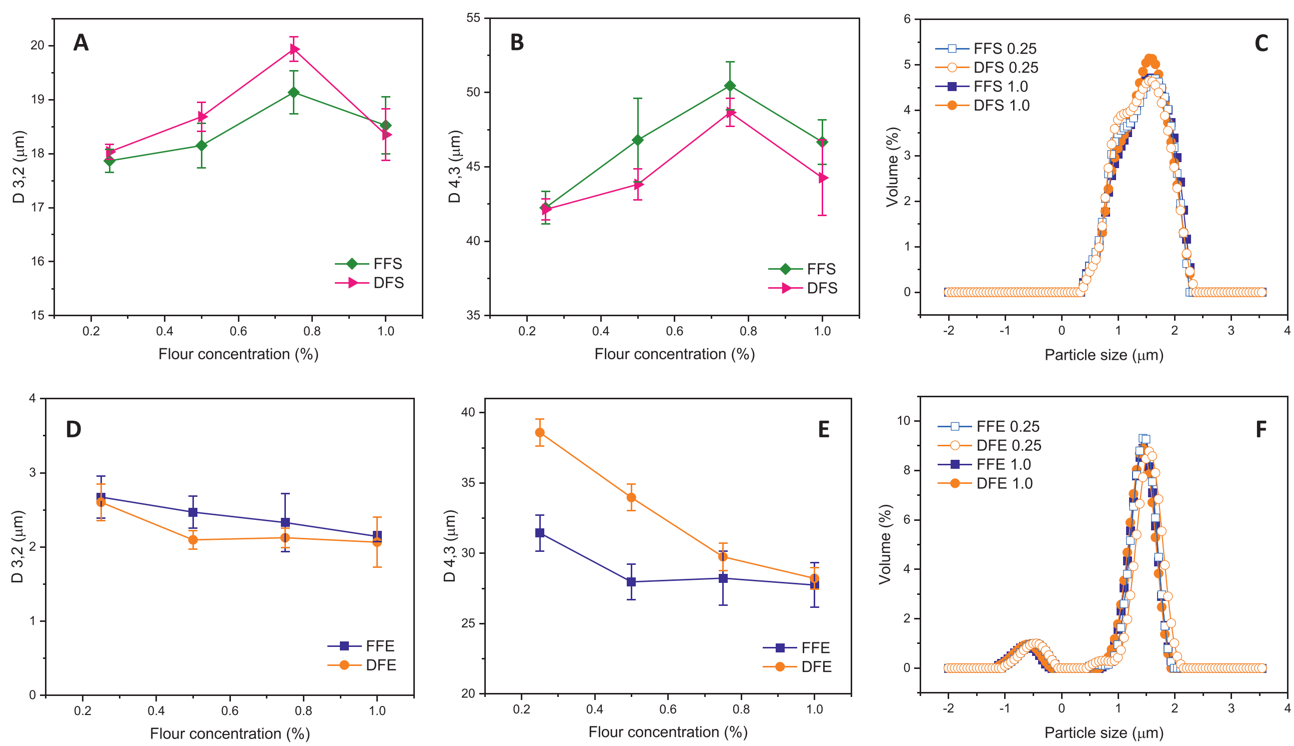

Fig. 6. Surface mean diameter d_{32} (μm) and volume mean diameter d_{43} (μm) of (A) FFS, (B) DFS, (D) FFE and (E) DFE as a function of concentrations (0.25%, 0.5%, 0.75% and 1.0%) of flour of narrow-leafed lupin. Droplet size distribution profiles of (C) FFS and DFS and (F) FFE and DFE at concentrations of 0.25% and 1.0% of flour of narrow-leafed lupin. All measurements were made immediately after preparation of the suspensions and emulsions. Vertical error bars represent the standard deviation of the means ($n = 3$).

there was a risk of clogging the laboratory microfluidizer at higher flour concentration (>2%). The composition of the lupin flour emulsions with their estimated protein content is shown in Table 3.

FFS had lower surface mean diameter (d_{32}) and higher volume mean diameter (d_{43}) than DFS (Fig. 6A and B). The highest droplet sizes in suspension were found in the 0.75% concentration (d_{32} = ~19 μm in FFS and ~20 μm in DFS; d_{43} = ~50 μm and ~49 μm, respectively). Droplet sizes were similarly small in the 0.25% and 1.0% concentrations of both FFS and DFS (d_{32} = ~18 μm; d_{43} = ~42 – 46 μm), but the size distribution was narrower in the 1.0% samples than in the 0.25% ones (Fig. 6C). All of the peaks showed a shoulder at a diameter about 10 μm (Fig. 6C). Particle size of the suspension is important because it influences the emulsifying ability, physical and chemical stability of the future applications (Lo et al., 2021). The smallest droplets are usually the most stable over time because of their lower settling speed (McClements, 2007).

The oil droplets of the emulsions were smaller and more stable than the particles of the corresponding suspensions. The average oil droplet sizes of the emulsions (d_{32} and d_{43}) decreased with increasing flour concentrations. The emulsions with the lowest flour concentration had the largest individual oil droplets (d_{32} = ~2.6 μm; d_{43} = ~31 in FFE and ~39 μm in DFE). Similarly, pea flour emulsion showed a decrease in oil droplet size at higher protein concentration (≥ 0.2 wt%) (Sridharan et al., 2020). At lower flour concentration (≤ 0.5%), there were insufficient quantities of particles to cover the large fraction of oil droplets present (5%). In this condition, good homogenization did not ensure better emulsification or stabilization.

Particle size distributions of FFE 1.0% and DFE 1.0% presented a shoulder peak while particle size distributions of FFE 0.25% and DFE 0.25% displayed two shoulder peaks (multi-modal distribution; Fig. 6F). The presence of the shoulder peak in high flour concentration indicated the existence of non-emulsified materials such as various sizes of cell wall materials (insoluble polysaccharides).

The ζ-potential of FFS and DFS decreased with the increasing flour concentrations (0.25% to 1.0%) (Fig. 7A) and values were greater in FFS than DFS. According to Walstra (2003), a dispersion with ζ-potential value of ±25 mV is electrostatically stabilized, and none of these samples reached that value. A suspension of lupin protein isolate at pH 7 had a ζ-potential of -35 mV and the value increased to -28 mV when heated to 121 °C (Berghout et al., 2015b). Since our flour was not fractionated, the ζ-potential values could have been affected by the high concentration of polysaccharides in the suspensions.

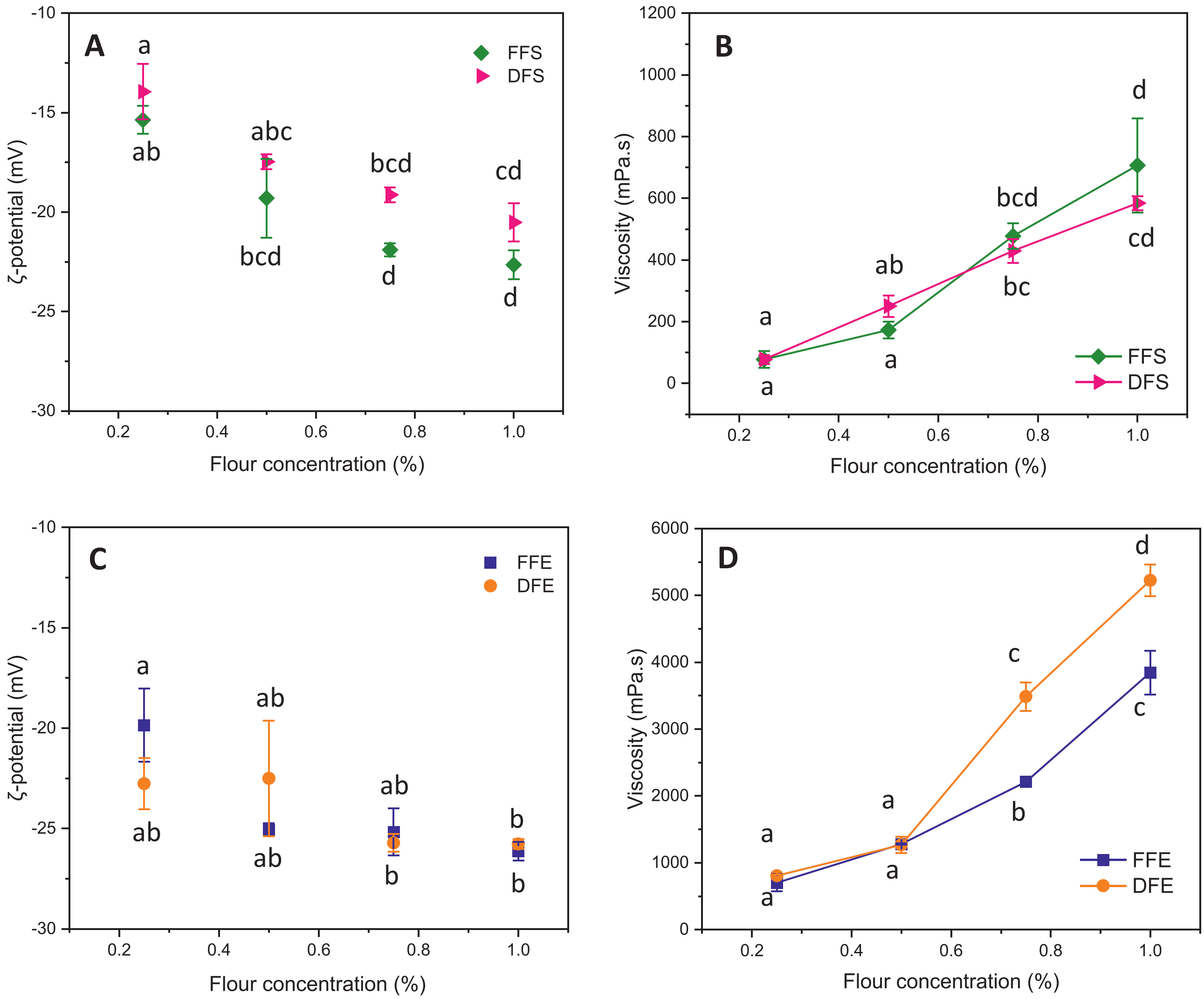

Fig. 7. ζ-potential and viscosity (at shear rate 10 s^{-1}) of FFS and DFS samples (A and B), and, FFE and DFE samples (C and D) at different flour concentrations (0.25%, 0.5%, 0.75% and 1.0%). Vertical error bars represent the standard deviation of the means ($n = 2$). Different lowercase letters in the figures indicate significant differences ($p < 0.05$).

Similarly, the ζ-potential values of the emulsions decreased with the increasing flour concentrations. The emulsions with higher flour concentrations (0.75% and 1.0%) were more negatively charged and hence more electrostatically stable than those at the lower flour concentrations. The proteins and fibre components were adsorbed on the oil-water interface, providing a layer with electrostatic and/or steric repulsive forces between emulsion droplets, thus stabilizing the emulsion systems. No significant difference ($p < 0.05$) in ζ-potential was observed between FFE and DFE samples at the highest flour concentration (1%).

The impact of surface charge on suspension or emulsion stability is also related to viscosity. At a shear rate of 10 s^{-1}, the viscosity values of FFS and DFS samples increased with the increase of flour concentrations (Fig. 7B). This is due to the increased protein-fibre interactions in the aqueous solutions at higher flour concentrations. In other legumes (e.g., pea, soybean and lentil), starch is the main contributor to the thickening ability of the suspension or emulsion (Sridharan et al., 2020; Pasqualone et al., 2021; Zhao et al., 2021). Since lupin samples have very low starch content, the main thickening agent in their suspension and emulsion systems is concluded to be pectin (Fig. 1 and 2).

The viscosity of the emulsions (Fig. 7D) was much higher than that of the corresponding suspensions. The presence of oil droplets in the emulsions increases the protein-fibre-oil interactions via hydrogen bonding and hydrophobic interactions, thus strengthening the emulsion matrix and leading to higher viscosity values (Johansson et al., 2021). The viscosity of the emulsions increased with increasing flour concentrations. At the two lower flour concentrations (0.25% and 0.5%), extensive oil droplet flocculation occurred due to insufficient coverage of the droplets by the protein and fibre materials, thus lowering the viscosity of the emulsions. At the higher concentrations, DFE viscosities were higher than those of FFE (2210–3716 mPa.s), and this was attributable to their higher water solubility and water-holding capacity.

TSI showed that FFS 1.0% was the most stable suspension (lowest TSI values during 7 days of storage time) followed by DFS 1.0% and FFS 0.75% (Fig. 8A). FFS 0.25% had the highest TSI values, so it was the least stable sample followed by DFS 0.25%. All of the suspensions showed phase separation (Fig. 8B) after 7 days of storage at room temperature and both DFS 0.25% to 0.75% showed a serum phase in addition to the aqueous and sedimentation phases. Cell wall fragments that may sediment during storage were visible in the suspension samples (Fig. 9) . In this situation, although the defatted flour suspension had higher solubility (Fig. 5) due to the exposure of active binding sites, the strength of the bonds with the water molecules may be weaker than those in full-fat flour suspensions, leading to faster destabilization of the DFS samples compared to the FFS samples.

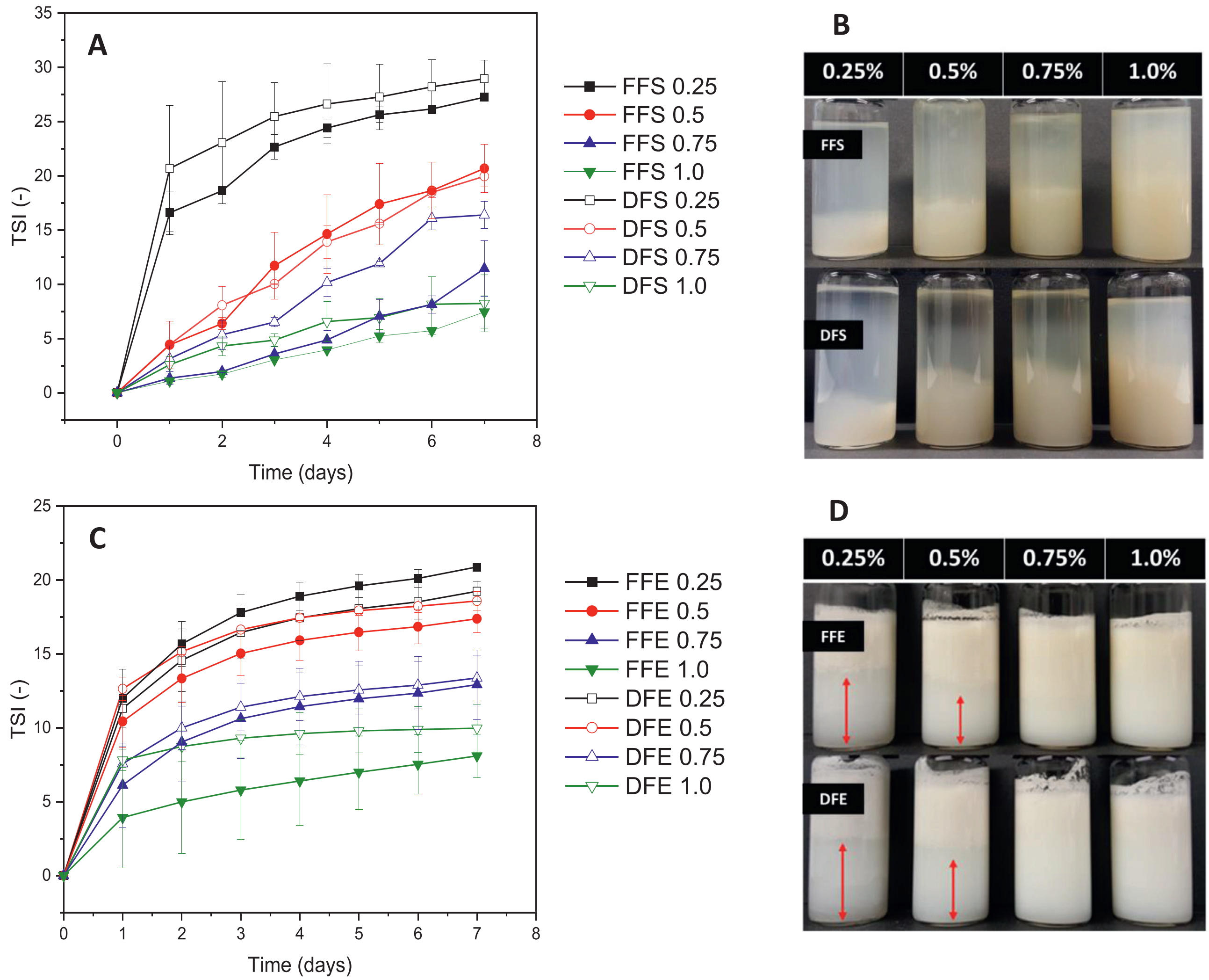

Fig. 8. Turbiscan stability index (TSI) as a function of time (days) during storage at room temperature of (A) suspensions (FFS and DFS) and (C) emulsions (FFE and DFE) made with different concentrations (0.25%, 0.5%, 0.75% and 1.0%) of flour of narrow-leafed lupin. Vertical error bars represent the standard deviation of the means ($n = 2$). Photographs of the (B) suspensions (FFS and DFS) and (D) emulsions (FFE and DFE) after 1 week of storage at room temperature. Double-headed arrows in D show emulsion phase separated from the creaming phase.

The emulsions showed some similarities to the suspensions in the TSI analysis. Higher concentrations were more stable than lower concentrations, but in this case, the full-fat samples were more stable than the defatted ones except at the lowest concentration (Fig. 8C). All emulsion samples showed phase separation into creaming and emulsion phases after 7 days of storage at room temperature (Fig. 8D). The formation of the creaming phase (an indication of droplet flocculation) was clearer at lower flour concentrations than at higher ones, due to the presence of larger oil droplets (Fig. 6D and E) that easily destabilize the emulsion during storage. These differences in oil droplet size were confirmed by microscopy (Fig. 9)

FFS 1.0% was thus the most stable suspension with the lowest TSI value (7.5; during 7 days of storage time; Fig. 8A), ζ-potential (-22.7 mV; Fig. 7A) and droplet size (d_{32} = ~18 µm; d_{43} = ~46 µm; Fig. 6A and B) along with the highest viscosity (707 mPa.s; Fig. 7B). This is attributable to the presence of more pectin at higher flour concentrations, which increases its thickening ability and contributes to the resistance of gravitational forces (sedimentation) during storage. Furthermore, at higher flour concentrations, the protein-fibre interaction was more electrostatically stable, further contributing to its stability. In the emulsion systems, FFE 1.0% was the most stable, with the lowest TSI value (8.1; during 7 days of storage time; Fig. 8B), ζ-potential (-26 mV; Fig. 7C) and droplet size (d_{32} = ~2.1 µm; d_{43} = ~28.0 µm; Fig. 6; D and E) along with high viscosity (~3800 mPa.s; Fig. 7D). Similarly to the suspension system, the higher viscosity at higher flour concentrations slowed down the phase separation (creaming). Compared to defatted emulsion samples, the full-fat emulsion samples were more stable due to stronger and more electrostatically stabilized protein-oil-polysaccharide interactions, caused by the higher solubility and water holding capacity in the samples (Fig. 5A and B).

This study has demonstrated the possibility to produce stable oil-in-water emulsion from the flour of whole lupin seeds without further fractionation of its components. Dehulling and milling of lupin seeds, then defatting the flour and subjecting it to a wet fractionation process, involves considerable water, chemical and energy inputs so its environmental sustainability is questionable (Berghout et al., 2015b). This study has also showed that the fibre fraction from the whole lupin seed contributed to the emulsion stability. Flour concentrations higher than 2.0% may clog the microfluidization step due to the high content of cell wall materials. Joseph et al. (2020) found that > 3 wt% of lupin hull powder can create very firm gels and clog a microfluidizer. However, an industrial-scale microfluidizer (ISM) can further increase the solubility of legume flours (He et al., 2021). The results in this study demonstrated the possibility to support sustainability by utilizing flour from the whole

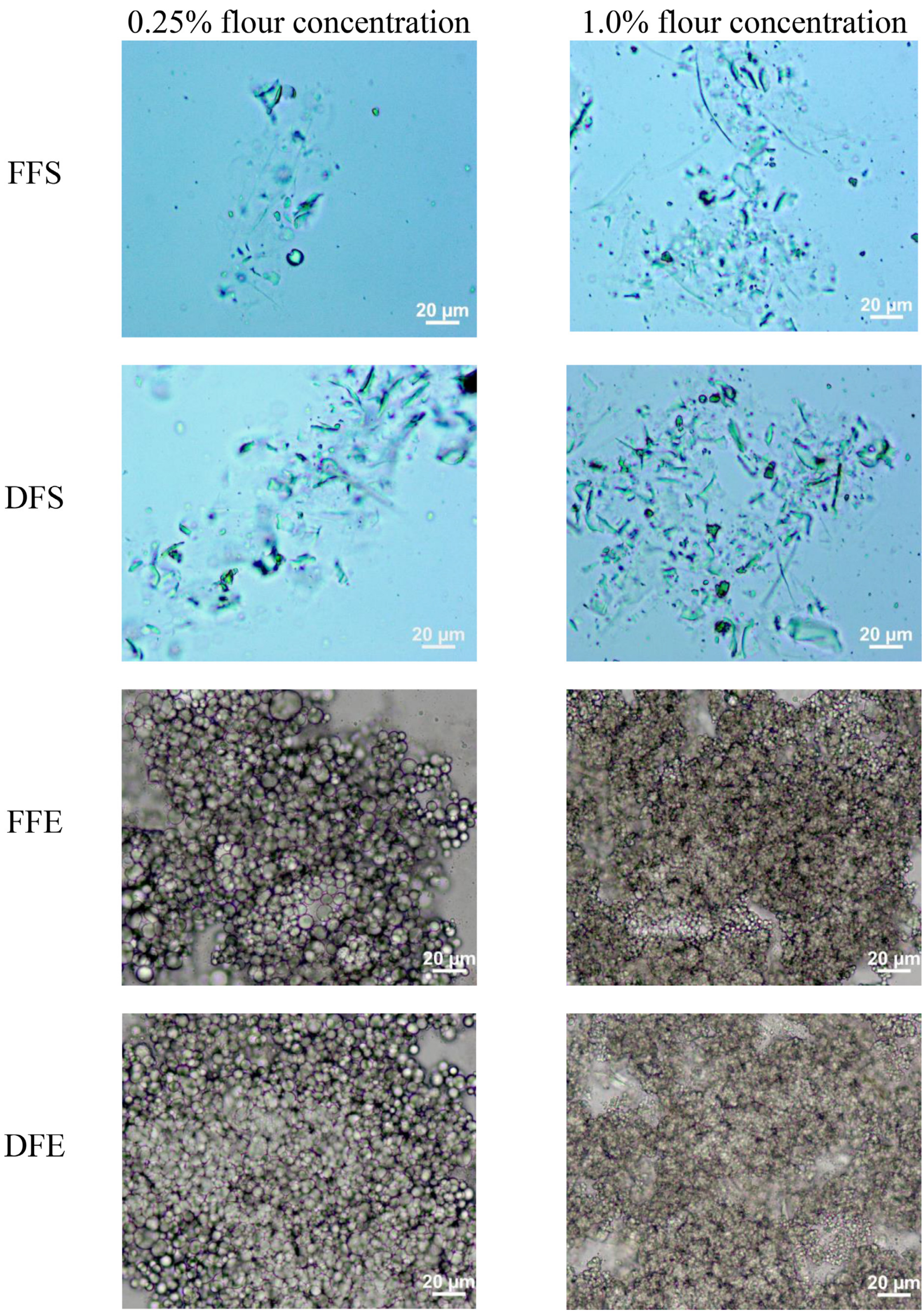

Fig. 9. Micrographs of selected suspensions (FFS and DFS) and emulsions (FFE and DFE) made with different concentrations (0.25% and 1.0%) of flour from narrow-leafed lupin. Magnification was 40 × . Scale bars correspond to 20 µm.

seed in future industrial applications (e.g., food, cosmetics and pharmaceuticals).

4. Conclusion

Lupins have a higher content of fibre than most other crops. Sugar analysis indicated that the main polysaccharide in the fibre fraction (enzymatically fractionated) is a pectin having homogalacturonan and rhamnogalacturonan-I domains. The presence of rhamnogalacturonan-I, with branches of galactan and arabinan, is in line with the existing model of lupin fibre structure but the presence of a linear and unbranched (homogalacturonan) region is novel. For the efficient valorization of lupin, a better understanding of its chemical and nutritional attributes is vital, including the polysaccharide, protein and fat fractions. In addition, this study physically characterized both whole seed full-fat lupin flour (unrefined) and defatted lupin flour (minimally refined) in dispersion and emulsion phases. The solubility and water holding capacity of the flours increased significantly with mechanical treatments (high-speed and high-pressure homogenization). Stable oil-in-water emulsions were produced using unrefined and minimally refined lupin flour, despite the presence of non-protein materials (insoluble and soluble polysaccharides). Suspensions and emulsions at higher flour concentrations (0.75% and 1.0%) were more stable than those at lower concentrations (0.25% and 0.5%). The insights from this study can enhance the use of unrefined whole lupin seed as emulsifiers, leading to simpler and more sustainable processing steps during the production of future industrial applications.

Statement

This research does not involve any human or animal studies.

Declaration of Competing Interest

The authors declare that they have no known competing financial interests or personal relationships that could have appeared to influence the work reported in this paper.

CRediT authorship contribution statement

Anis N. Arzami: Conceptualization, Methodology, Formal analysis, Investigation, Writing – original draft, Writing – review & editing, Visualization. **Danila Morais de Carvalho:** Conceptualization, Methodology, Formal analysis, Investigation, Writing – original draft, Writing – review & editing, Visualization. **Francisco Vilaplana:** Conceptualization, Methodology, Formal analysis, Investigation, Writing – review & editing, Visualization. **Frederick L. Stoddard:** Conceptualization, Methodology, Writing – review & editing, Supervision. **Kirsi S. Mikkonen:** Conceptualization, Methodology, Writing – review & editing, Supervision.

Data Availability

Data will be made available on request.

Acknowledgments

We would like to thank Katerina Zitkova and Marianna Koivisto for their technical support in this study. This work was financially supported by Faculty of Agriculture and Forestry at University of Helsinki under proof-of concept funding. The authors acknowledge Mr. Troy Faithfull for proofreading the manuscript.

Supplementary materials

Supplementary material associated with this article can be found, in the online version, at doi:10.1016/j.fufo.2022.100192.

References

Albersheim, P., Nevins, D.J., English, P.D., Karr, A., 1967. A method for the analysis of sugars in plant cell-wall polysaccharides by gas-liquid chromatography. Carbohydr. Res. 5, 340–345. doi:10.1016/S0008-6215(00)80510-8.

Berghout, J.A.M., Boom, R.M., van der Goot, A.J., 2014. The potential of aqueous fractionation of lupin seeds for high-protein foods. Food Chem. 159, 64–70. doi:10.1016/j.foodchem.2014.02.166.

Berghout, J.A.M., Boom, R.M., van der Goot, A.J., 2015a. Understanding the differences in gelling properties between lupin protein isolate and soy protein isolate. Food Hydrocoll. 43, 465–472. doi:10.1016/j.foodhyd.2014.07.003.

Berghout, J.A.M., Venema, P., Boom, R.M., van der Goot, A.J., 2015b. Comparing functional properties of concentrated protein isolates with freeze-dried protein isolates from lupin seeds. Food Hydrocoll. 51, 346–354. doi:10.1016/j.foodhyd.2015.05.017.

Bian, J., Peng, F., Xu, F., Sun, R.-C., Kennedy, J.F., 2010. Fractional isolation and structural characterization of hemicelluloses from *Caragana korshinskii*. Carbohydr. Polym. 80, 753–760. doi:10.1016/j.carbpol.2009.12.023.

Buckeridge, M.S., dos Santos, H.P., Tiné, M.A.S., 2000. Mobilisation of storage cell wall polysaccharides in seeds. Plant Physiol. Biochem. 38, 141–156. doi:10.1016/S0981-9428(00)00162-5.

Byg, I., Diaz, J., Øgendal, L.H., Harholt, J., Jørgensen, B., Rolin, C., Svava, R., Ulvskov, P., 2012. Large-scale extraction of rhamnogalacturonan I from industrial potato waste. Food Chem 131, 1207–1216. doi:10.1016/j.foodchem.2011.09.106.

Ciucanu, I., Kerek, F., 1984. A simple and rapid method for the permethylation of carbohydrates. Carbohydr. Res. 31, 209–217. doi:10.1016/0008-6215(84)85242-8.

Chaikumpollert, O., Methacanon, P., Suchiva, K., 2004. Structural elucidation of hemicelluloses from Vetiver grass. Carbohydr. Polym. 57, 191–196. doi:10.1016/j.carbpol.2004.04.011.

De Visser, C.L.M., Schreuder, R., Stoddard, F.L., 2014. The EU's dependency on soya bean import for the animal feed industry and potential for EU produced alternatives. OCL 21, D407. doi:10.1051/ocl/2014021.

Egaña, J.I., Uauy, R., Cassorla, X., Barrera, G., Yañez, E, 1992. Sweet lupin protein quality in young men. J. Nutr. 122, 2341–2347. doi:10.1093/jn/122.12.2341.

Feedipedia. (2022). Animal feed resources information system. www.feedipedia.org, (accessed 13 January 2022)

Gupta, S., Madan, R.N., Bansal, M.C., 1987. Chemical composition of *Pinus caribaea* hemicellulose. Tappi J. 70, 113–114.

Harholt, J., Suttangkakul, A., Scheller, H.V., 2010. Biosynthesis of pectin. Plant Physiol. 153, 384–395. doi:10.1104/pp.110.156588.

He, X., Chen, J., He, X., Feng, Z., Li, C., Liu, W., Dai, T., Liu, C., 2021. Industry-scale microfluidization as a potential technique to improve solubility and modify structure of pea protein. Innov. Food Sci. Emerg. Technol. 67, 102582. doi:10.1016/j.ifset.2020.102582.

Jayasena, V., Chih, H.J., Nasar-Abbas, S., 2011. Efficient isolation of lupin protein. Food Aust. 63, 306–309.

Johansson, M., Xanthakis, E., Langton, M., Menzel, C., Vilaplana, F., Johansson, D.P., Lopez-Sanchez, P., 2021. Mixed legume systems of pea protein and unrefined lentil fraction: Textural properties and microstructure. LWT 144, 111212. doi:10.1016/j.lwt.2021.111212.

Joseph, C., Savoire, R., Harscoat-Schiavo, C., Pintori, D., Monteil, J., Faure, C., Leal-Calderon, F., 2020. Pickering emulsions stabilized by various plant materials: Cocoa, rapeseed press cake and lupin hulls. LWT 130, 109621. doi:10.1016/j.lwt.2020.109621.

Lammi, C., Aiello, G., Vistoli, G., Zanoni, C., Arnoldi, A., Sambuy, Y., Ferruzza, S., Ranaldi, G., 2016. A multidisciplinary Investigation on the bioavailability and activity of peptides from lupin protein. J. Funct. Foods. 24, 297–306. doi:10.1016/j.jff.2016.04.017.

Lizarazo, C.I., Lampi, A.-M., Liu, J., Sontag-Strohm, T., Piironen, V., Stoddard, F.L., 2015. Nutritive quality and protein production from grain legumes in a boreal climate. J. Sci. Food Agric. 95, 2053–2064. doi:10.1002/jsfa.6920, Corrigendum *J. Sci. Food Agric.* 97, 1962. doi.org/10.1002/jsfa.8213.

Lizarazo, C.I., Yli-Halla, M., Stoddard, F.L., 2016. Pre-crop effects on the nutrient composition and utilization efficiency of faba bean (*Vicia faba* L.) and narrow-leafed lupin (*Lupinus angustifolius* L.). Nutr. Cycling Agroecosyst. 103, 311–327. doi:10.1007/s10705-015-9743-0.

Lo, B., Kasapis, S., Farahnaky, A., 2021. Lupin protein: Isolation and techno-functional properties, a review. Food Hydrocoll. 112, 106318. doi:10.1016/j.foodhyd.2020.106318.

Lqari, H., Vioque, J., Pedroche, J., Millán, F., 2002. Lupinus angustifolius protein isolates: chemical composition, functional properties and protein characterization. Food Chem. 76, 349–356. doi:10.1016/S0308-8146(01)00285-0.

Lucas, M.M., Stoddard, F., Annicchiarico, P., Frias, J., Martinez-Villaluenga, C., Süssmann, D., Duranti, M., Seger, A., Zander, P., Pueyo, J., 2015. The future of lupin as a protein crop in Europe. Front. Plant Sci. 6. doi:10.3389/fpls.2015.00705.

LupinFoods. (2022). Lupin flake. http://www.lupinfoods.com.au/shop/(accessed 8 February 2022).

Mariotti, F., Pueyo, M.E., Tomé, D., Mahé, S., 2007. The bioavailability and postprandial utilisation of sweet lupin (Lupinus albus)-flour protein is similar to that of purified soyabean protein in human subjects: a study using intrinsically 15N-labelled proteins. Br. J. Nutr. 87, 315–323. doi:10.1079/BJN2002526.

McClements, D.J., 2007. Critical review of techniques and methodologies for characterization of emulsion stability. Crit. Rev. Food Sci. Nutr. 47, 611–649. doi:10.1080/10408390701289292.

Miao, Z.H., Fortune, J.A., Gallagher, J., 2001. Anatomical structure and nutritive value of lupin seed coats. Aust. J. Agric. Res. 52, 985–993. doi:10.1071/AR00117.

Mohammed, M.A., Mohamed, E.A., Yagoub, A.E.A., Mohamed, A.R., Babiker, E.E., 2017.

Effect of processing methods on alkaloid, phytate, phenolics, antioxidants activity and minerals of newly developed lupin (*Lupinus albus* L.) cultivar. J. Food Process. Preserv. 41, e12960. doi:10.1111/jfpp.12960.

Morais de Carvalho, D., Martínez-Abad, A., Evtuguin, D.V., Colodette, J.L., Lindström, M.E., Vilaplana, F., Sevastyanova, O., 2017. Isolation and characterization of acetylated glucuronoarabinoxylanfrom sugarcane. Carbohydr. Polym. 156, 223–234. doi:10.1016/j.carbpol.2016.09.022.

Naumann, S., Schweiggert-Weisz, U., Martin, A., Schuster, M., Eisner, P., 2021. Effects of extrusion processing on the physiochemical and functional properties of lupin kernel fibre. Food Hydrocoll. 111, 106222. doi:10.1016/j.foodhyd.2020.106222.

Pasqualone, A., Costantini, M., Labarbuta, R., Summo, C., 2021. Production of extruded-cooked lentil flours at industrial level: effect of processing conditions on starch gelatinization, dough rheological properties and techno-functional parameters. LWT 147, 111580. doi:10.1016/j.lwt.2021.111580.

Peng, W., Kong, X., Chen, Y., Zhang, C., Yang, Y., Hua, Y., 2016. Effects of heat treatment on the emulsifying properties of pea proteins. Food Hydrocoll. 52, 301–310. doi:10.1016/j.foodhyd.2015.06.025.

Pollard, N.J., Stoddard, F.L., Popineau, Y., Wrigley, C.W., MacRitchie, F., 2002. Lupin flours as additives: dough mixing, breadmaking, emulsifying and foaming. Cereal Chem. 79, 662–669. doi:10.1094/CCHEM.2002.79.5.662.

Porres, J.M., Aranda, P., López-Jurado, M., Urbano, G, 2007. Nutritional evaluation of protein, phosphorus, calcium and magnesium bioavailability from lupin (*Lupinus albus* var. multolupa)-based diets in growing rats: effect of α-galactoside oligosaccharide extraction and phytase supplementation. Br. J. Nutr. 95, 1102–1111. doi:10.1079/BJN20061771.

Raymundo, A., Franco, J.M., Empis, J., Sousa, I., 2002. Optimization of the composition of low-fat oil-in-water emulsions stabilized by white lupin protein. J. Am. Oil Chem. Soc. 79, 783–790. doi:10.1007/s11746-002-0559-6.

Rosenbohm, C., Lundt, I., Christensen, T.M.I.E., Young, N.W.G., 2003. Chemically methylated and reduced pectins: preparation, characterisation by ^{1}H NMR spectroscopy, enzymatic degradation, and gelling properties. Carbohydr. Res. 338, 637–649. doi:10.1016/S0008-6215(02)00440-8.

Sathe, S., Deshpande, S., Salunkhe, D., 1982. Functional properties of lupin seed (*Lupinus mutabilis*) proteins and protein concentrates. J. Food Sci. 47, 491–497. doi:10.1111/j.1365-2621.1982.tb10110.x.

Sipsas, S., 2008. Lupin products - concepts and reality. In: Lupins for health and wealth, Proceedings of the 12th International Lupin Conference, Fremantle, Western Australia. International Lupin Association, pp. 506–513 14-18 September 2008.

Sironi, E., Sessa, F., Duranti, M., 2005. A simple procedure of lupin seed protein fractionation for selective food applications. Eur. Food Res. Technol. 221, 145–150. doi:10.1007/s00217-005-1151-2.

Sridharan, S., Meinders, M.B.J., Bitter, J.H., Nikiforidis, C.V., 2020. Pea flour as stabilizer of oil-in-water emulsions: Protein purification unnecessary. Food Hydrocoll. 101, 105533. doi:10.1016/j.foodhyd.2019.105533.

Sujak, A., Kotlarz, A., Strobel, W., 2006. Compositional and nutritional evaluation of several lupin seeds. Food Chem. 98, 711–719. doi:10.1016/j.foodchem.2005.06.036.

Sun, J.X., Sun, X.F., Sun, R.C., Su, Y.Q., 2004. Fractional extraction and structural characterization of sugarcane bagasse hemicelluloses. Carbohydr. Polym. 56, 195–204. doi:10.1016/j.carbpol.2004.02.002.

Sundberg, A., Sundberg, K., Lillandt, C., Holmbom, B., 1996. Determination of hemicelluloses and pectins in wood and pulp fibres by acid methanolysis and gas chromatography. Nord. Pulp Pap. Res. J. 11, 216–219. doi:10.3183/npprj-1996-11-04-p216-219, 226.

Süssmann, D., Pickardt, C., Schweiggert, U., Eisner, P., 2013. Influence of different processing parameters on the isolation of lupin (*Lupinus Angustifolius* L.) protein isolates: a preliminary study. J. Food Process Eng. 36, 18–28. doi:10.1111/j.1745-4530.2011.00647.x.

Thakur, B.R., Singh, R.K., Handa, A.K., Rao, M.A., 1997. Chemistry and uses of pectin - a review. Crit. Rev. Food Sci. Nutr. 37 (1), 47–73. doi:10.1080/10408399709527767.

Thambiraj, S.R., Phillipsa, M., Koyyalamudic, S.R., Reddy, N., 2018. Yellow lupin (*Lupinus luteus* L.) polysaccharides: antioxidant, immunomodulatory and prebiotic activities and their structural characterization. Food Chem. 267, 319–328. doi:10.1016/j.foodchem.2018.02.111.

Tucek, M. 2006. Use of lupin bran in high-fibre food products. US Patent 20090285961A1.

Turnbull, C.M., Baxter, A.L., Johnson, gt, Stuart, K, 2005. Water-binding capacity and viscosity of Australian sweet lupin kernel fibre under in vitro conditions simulating the human upper gastrointestinal tract. Int. J. Food Sci. Nutr. 56, 87–94. doi:10.1080/09637480500081080.

Walstra, P., 2003. Colloidal Interactions, in: Physical Chemistry of Foods. Marcel Dekker Inc., New York, pp. 455–493.

Winning H., Viereck, N., Nørgaard, L., Larsenb, J., & Engelsen, S. B. 2007. Quantification of the degree of blockiness in pectins using 1H NMR spectroscopy and chemometrics. Food Hydrocoll.. 21, 256-26. https://doi.org/10.1016/j.foodhyd.2006.03.017.

Xu, C., Leppänen, A.-S., Eklund, P., Holmlund, P., Sjöholm, R., Sundberg, K., Willför, S., 2010. Acetylation and characterization of spruce (*Picea abies*) galactoglucomannans. Carbohydr. Res. 345, 810–816. doi:10.1016/j.carres.2010.01.007.

Yang, L., Zang, L-M., 2009. Chemical structural and chain conformational characterization of some bioactive polysaccharides isolated from natural sources. Carbohydr. Polym. 76, 349–361. doi:10.1016/j.carbpol.2008.12.015.

Zhao, Q., Tian, H., Chen, L., Zeng, M., Qin, F., Wang, Z., He, Z., Chen, J, 2021. Interactions between soluble soybean polysaccharide and starch during the gelatinization and retrogradation: effects of selected starch varieties. Food Hydrocoll. 118, 106765. doi:10.1016/j.foodhyd.2021.106765.

Zhong, L., Fang, Z., Wahlqvist, M.L., Wu, G., Hodgson, J.M., Johnson, S.K, 2018. Seed coats of pulses as a food ingredient: characterization, processing, and applications. Trends Food Sci. Technol. 80, 35–42. doi:10.1016/j.tifs.2018.07.021.

Zhi, Z., Chen, J., Li, S., Wang, W., Huang, R., Liu, D., Ding, T., Linhardt, R. J., Chen, S., Ye, X., 2017. Fast preparation of RG-I enriched ultra-low molecular weight pectin by an ultrasound accelerated Fenton process. Scientific Reports 7, 541. doi:10.1038/s41598-017-00572-3.

Zhong, L., Fang, Z., Wahlqvist, M.L., Hodgson, J.M., Johnson, S.K, 2019. Extrusion cooking increases soluble dietary fibre of lupin seed coat. LWT 99, 547–554. doi:10.1016/j.lwt.2018.10.018.

Øbro, J., Harholt, J., Scheller, H.V., Orfila, C., 2004. Rhamnogalacturonan I in *Solanum tuberosum* tubers contains complex arabinogalactan structures. Phytochem 65, 1429–1438. doi:10.1016/j.phytochem.2004.05.002.